



Efficient blue-emitting molecules by incorporating sulfur-containing moieties into triarylcyclopentadiene: Synthesis, crystal structures and photophysical properties



Junwei Ye ^a, Yuan Gao ^a, Lei He ^a, Tingting Tan ^a, Wei Chen ^a, Yu Liu ^{b, **}, Yue Wang ^b, Guiling Ning ^{a, *}

^a State Key Laboratory of Fine Chemicals and School of Chemical Engineering, Dalian University of Technology, 2 Linggong Road, Dalian 116012, PR China

^b State Key Laboratory of Supramolecular Structure and Materials, College of Chemistry, Jilin University, Changchun 130012, PR China

ARTICLE INFO

Article history:

Received 27 April 2015

Received in revised form

7 August 2015

Accepted 7 September 2015

Available online 30 September 2015

Keywords:

Blue-emitting molecules

Triarylcyclopentadiene

Thiophene

Aggregation-induced emission

enhancement

Crystal structures

Organic light emitting diode

ABSTRACT

Three highly fluorescent blue-emitting molecules, namely 1,2-diphenyl-4-(4-thiophenyl)-1,3-cyclopentadiene (**DPCP 1**), 1,2-diphenyl-4-(4-thiophenyl)phenyl)-1,3-cyclopentadiene (**DPCP 2**) and 1,2-diphenyl-4-(4-dibenzothienyl)phenyl)-1,3-cyclopentadiene (**DPCP 3**), have been synthesized by using aryl-substituted cyclopentadiene and thiophene or dibenzothienophene as ingredients. The single crystal structure analysis reveals that **DPCP 1–3** are non-coplanar structures and bulky substituents on cyclopentadiene core imposed a significant reduction on intermolecular interactions, hence leading to their intense blue emission in both solution and solid state. **DPCP 1** and **DPCP 3** also showed a typical aggregation-induced emission enhancement in mixed water/acetone solution. These compounds exhibited good thermal stability with decomposition temperatures between 239 and 383 °C. The non-doped organic light-emitting diodes using **DPCP 3** as the emitting layer displayed a very low turn-on voltage at 3.2 V and pure blue emission with the Commission Internationale de l'Éclairage (CIE_{x,y}) coordinates of (0.16, 0.16) and a maximum luminance of 2277 cd m⁻².

© 2015 Elsevier Ltd. All rights reserved.

1. Introduction

The development of high efficient organic optoelectronic materials has attracted tremendous attention from both the academic and industrial research communities because of their promising applications in the fields of organic light-emitting diodes (OLEDs) [1], illumination [2], photovoltaic cells [3], molecular probes [4], bio-labeling [5] and photonic devices [6]. Most of organic fluorophores are highly emissive in their dilute solutions, but it becomes weakly luminescent when fabricated into thin films. In the solid state, the molecules aggregate to form less emissive species such as excimers, leading to a reduction in the luminescence efficiency [7]. Such aggregation-caused quenching (ACQ) effect has become a drawback to the development of high efficient and stable OLEDs [8]. Since the anti-ACQ compounds 1-methyl-1,2,3,4,5-

pentaphenylsilole and 1-cyano-*trans*-1,2-bis-(4'-methylbiphenyl) ethylene having strong emission in the aggregated state than that in dilute solution were reported by Tang et al. [9] and Park et al. [10], respectively, different type of materials with aggregation-induced emission (AIE) or aggregation induced emission enhancement (AIEE) characteristics have been discovered [11]. The restriction of intermolecular rotations (RIR), molecular planarization, prevention of exciton diffusion and *J*-aggregates formation effects are accepted to understand enhanced emission phenomena [12]. However, the efficient AIE or AIEE materials systems for blue-emitting molecules are still quite limited.

In order to decrease the aggregation quenching of aromatic hydrocarbons possessing extended π -conjugation and planar skeleton, some efforts have been spent to modify the fluorophore backbone by attaching bulky substituents to the molecular core [13]. For examples, a series of aryl-functionalized blue emitting pyrene derivatives were synthesized by steric hindrance introduced through bulky substituents in its 1-, 3-, 5-, 6-, 8- and 9H position of pyrene core [14], respectively. Several quinacridone derivatives with high-emission property in both solution and solid

* Corresponding author. Fax: +86 411 84986065.

** Corresponding author.

E-mail addresses: yuliu@jlu.edu.cn (Y. Liu), ninggl@dlut.edu.cn (G. Ning).

state were synthesized based on the introduction of two propeller-like pentaphenyl groups to a quinacridone core [15]. Furthermore, cyclopentadiene derivatives (CPs) are known for versatile organic molecules due to their good electrical and optical properties [16,17], as well as multicolor emission in nano-aggregation [18]. Huang et al. [19] reported two CPs named 1,2,3,4-tetraphenyl-1,3-cyclopentadiene (TPCP) and 1,2,3,4,5-pentaphenyl-1,3-cyclopentadiene (PPCP) which were used in blue light-emitting OLEDs. Yoshino et al. [20] reported multicolor OLEDs based on PPCP or PPCP-doped poly(3-alkylthiophene) as emissive layer. Recently, our researches are mainly focused on the molecule design and understanding relationship between molecular structures and optoelectronic properties of the polyphenyl substituted CPs, and a new class of triarylsubstituted CPs with good thermal stability and strong fluorescence in solid state were synthesized [21]. It has been demonstrated that the introduction of rich electron-donor moieties into the molecular backbone of CPs would improve the emission efficiency and color purity of the target molecules.

In this work, we would like to introduce thiophene and dibenzothiothiophene segments with the good amorphous film forming ability and the electron-transporting ability [22] into the 4-position of the 1,2-diphenyl or 1, 2, 4-triphenyl cyclopentadienyl core to obtain a series of novel blue emission materials, namely 1,2-diphenyl-4-thiophenyl-1,3-cyclopentadiene (**DPCP 1**), 1,2-diphenyl-4-(4-thiophenyl)phenyl-1,3-cyclopentadiene (**DPCP 2**) and 1,2-diphenyl-4-(4-dibenzothiothiophenyl)phenyl-1,3-cyclopentadiene (**DPCP 3**). We present a comprehensive investigation on these three CPs compounds, which not only encompasses their thermal, photophysical and electrochemical properties, but also the emphatically studies on their single-crystal structures and DFT calculation have been investigated to understand the relationship between chemical structures and luminescent properties. The resulting non-coplanar structures due to the steric hindrance of bulky phenyl ring and sulfur-containing moieties could suppress the intermolecular π - π interactions and reduce the aggregation formation. It is worth mentioning that an efficient pure blue OLEDs based on **DPCP 3** as the neat emitting layer was achieved.

2. Experimental section

2.1. Materials and methods

All reagents were analytical reagent grade and used as received. The solvents were purified with standard methods and dried as needed. All ^1H and ^{13}C NMR spectra were referenced to a Bruker AVANCE-400 MHz magnetic resonance spectrometer. HRMS were acquired on Micromass-GTC spectrometer. Differential scanning calorimetry (DSC) curves were obtained with a TA Instruments thermal analyzer (910S) at a heating rate of $10\text{ }^\circ\text{C min}^{-1}$ under nitrogen atmosphere. Thermogravimetric analyses (TGA) were performed with a METTLER TOLEDO (TGA/SDTA 851^e) under nitrogen atmosphere with a heating rate of $10\text{ }^\circ\text{C min}^{-1}$. UV absorption measurements were conducted on HITACHI U-4100 UV-vis Spectrophotometer. The photoluminescence (PL) studies were confirmed with a JASCO FP-6300 spectrofluorometer with a 150 W Xe lamp. The relative fluorescence quantum yields were estimated relative to solutions of $5 \times 10^{-5}\text{ M}$ quinine sulfate with $\Phi_{\text{F}} = 0.55$ in 0.1 M sulfuric acid solution as a standard sample [23]. Cyclic voltammetry (CV) measurement was carried out on a Shanghai Chenhua electrochemical workstation CHI660C in a three-electrode cell with a Pt disk working electrode, an Ag/AgCl reference electrode, and a glassy carbon counter electrode. All spectra were carried out at room temperature.

2.2. Synthesis

2.2.1. 1,2-Diphenyl-4-thiophenyl-1,3-cyclopentadiene (**DPCP 1**)

A solution of thiophene-2-carboxaldehyde (2.50 g, 22.29 mmol) and acetophenone (6.70 g, 55.83 mmol) in ethanol was heated to $65\text{ }^\circ\text{C}$, and aqueous sodium hydroxide (2.23 g, 55.83 mmol) was added to the solution. The mixture was heated to reflux for 1 h and then cooled to room temperature. The intermediate product was cyclized in Zn/CH₃COOH system for 5 h, in which zinc dusts were added per hour. The solution layer was poured into 600 mL water to get white precipitate. The solid was collected by filtration and then dried under vacuum, and it was dehydrated in the presence of concentrated hydrochloric acid for 3 h and then cooled to room temperature [19]. Light yellow solid precipitate was obtained by filtration. The obtained solid was purified by column chromatography on silica gel using dichloromethane/petroleum ether as eluent to obtain the product in yield 78%. ^1H NMR (400 MHz, CDCl₃) δ (ppm): 7.39–7.38 (m, 2H), 7.36–7.34 (m, 1H), 7.33–7.30 (m, 4H), 7.28–7.25 (m, 2H), 7.24–7.22 (m, 2H), 7.10–7.17 (m, 1H), 7.16–7.02 (m, 1H), 7.01–6.86 (m, 1H), 3.94 (s, 2H). ^{13}C NMR (100 MHz, CDCl₃) δ (ppm): 144.4, 144.3, 142.2, 139.5, 137.1, 136.8, 134.9, 132.9, 132.1, 128.5, 128.4, 128.3, 128.1, 127.8, 127.2, 126.6, 126.1, 125.3, 124.7, 122.9, 44.87. MS (API-ES): calcd for C₂₁H₁₆S, M: 300.1. Elem. Anal.: C, 83.98%; H, 5.42%; S, 10.71%. Found: C, 83.96%; H, 5.37%; S, 10.67%.

2.2.2. 1,2-Diphenyl-4-(4-thiophenyl)phenyl-1,3-cyclopentadiene (**DPCP 2**)

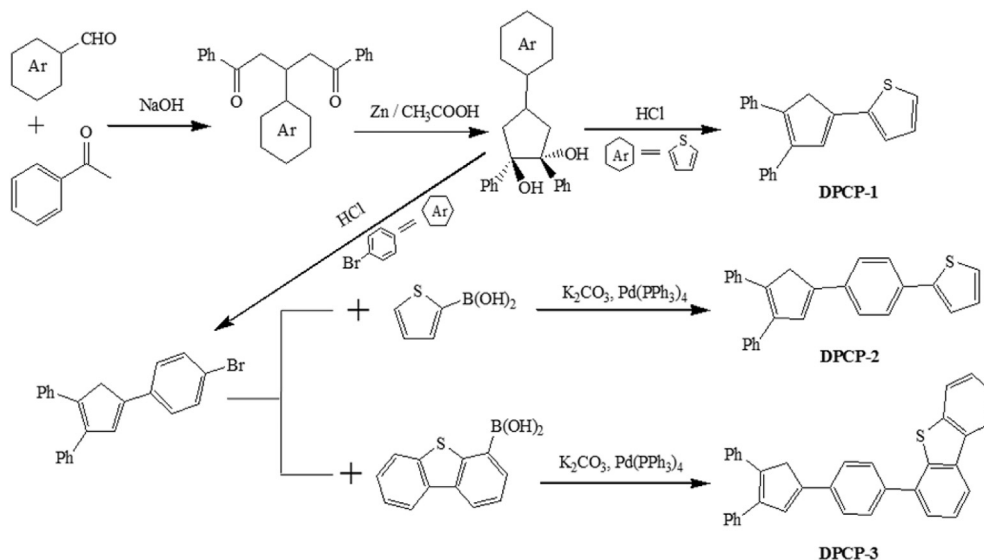
1,2-Diphenyl-4-(4-bromophenyl)-1,3-diene was synthesized according to our previously work [21] in essentially similar procedures. 1,2-diphenyl-4-(4-bromophenyl)-1,3-diene (0.78 g, 2.10 mmol) and the 2-thiopheneboronic acid (0.31 g, 2.40 mmol) in toluene (15 mL), 2 M aqueous K₂CO₃ solution (10 mL) and ethanol (5 mL) were added. The mixture was stirred for 30 min under an argon atmosphere at room temperature. Then the Pd(PPh₃)₄ catalyst was added and the reaction mixture was stirred at $80\text{ }^\circ\text{C}$ for 24 h allowing the temperature to decrease gradually to room temperature [14a,24]. The crude product was concentrated and purified by silica gel column chromatography using petroleum ether/dichloromethane (v:v, 10:1, yield 76%). ^1H NMR (400 MHz, CDCl₃) δ (ppm): 7.61–7.55 (m, 4H), 7.41–7.39 (m, 2H), 7.35–7.28 (m, 6H), 7.26–7.21 (m, 3H), 7.19–7.17 (m, 1H), 7.09–7.06 (m, 2H), 3.94 (s, 2H). ^{13}C NMR (100 MHz, CDCl₃) δ (ppm): 142.0, 140.4, 139.1, 138.1, 136.9, 136.6, 131.5, 128.5, 128.4, 128.3, 128.2, 127.7, 127.2, 126.6, 123.7, 122.8, 45.84. MS (API-ES): calcd for C₂₇H₂₀S, M: 376.1. Elem. Anal.: C, 86.21%; H, 5.39%; S, 8.63%. Found: C, 86.13%; H, 5.35%; S, 8.52%.

2.2.3. 1,2-Diphenyl-4-(4-dibenzothiothiophenyl)phenyl-1,3-cyclopentadiene (**DPCP 3**)

The synthesis of **DPCP 3** was similar to the above description for **DPCP 2** except that 2-thiopheneboronic acid was replaced by 4-dibenzothiothiopheneboronic acid. The light yellow powder was obtained with the yield of 85%. ^1H NMR (400 MHz, CDCl₃) δ (ppm): 8.23–8.21 (m, 1H), 8.19–8.17 (m, 1H), 7.88–7.86 (m, 1H), 7.79–7.74 (m, 4H), 7.59–7.57 (d, 1H), 7.56–7.54 (m, 1H), 7.51–7.49 (m, 2H), 7.46–7.44 (m, 2H), 7.39–7.34 (m, 5H), 7.32–7.29 (d, 1H), 7.27–7.25 (d, 1H), 7.22–7.21 (d, 1H), 7.16 (s, 1H), 4.04 (s, 2H). ^{13}C NMR (100 MHz, CDCl₃) δ (ppm): 144.5, 142.2, 139.7, 139.6, 139.1, 138.5, 137.2, 136.8, 136.7, 136.3, 135.8, 135.4, 132.4, 128.7, 128.6, 128.5, 128.3, 127.8, 127.3, 126.9, 126.8, 126.7, 125.3, 125.2, 124.4, 122.7, 121.8, 120.5, 45.0. MS (API-ES): calcd for C₃₅H₂₄S, M: 476.2. Elem. Anal.: C, 88.29%; H, 5.16%; S, 6.78%. Found: C, 88.20%; H, 5.08%; S, 6.73%.

2.2.4. Single-crystal X-ray crystallography

The single crystals of three compounds were grown from a mixture of CH₂Cl₂ and CH₃OH. X-ray crystal structure



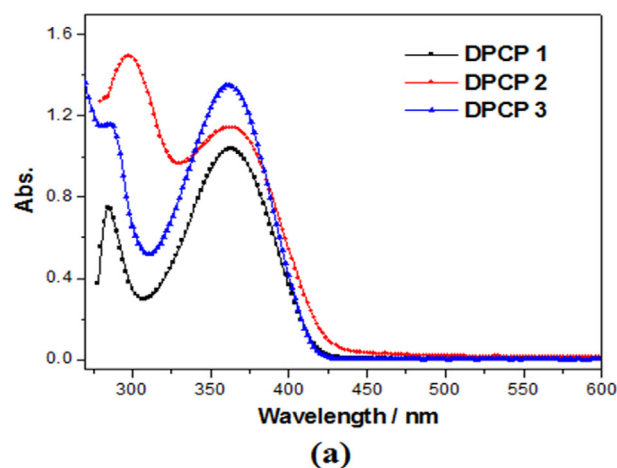
Scheme 1. Synthetic procedures and structures of DPCP 1–3.

determinations were performed on a Bruker SMART APEX CCD diffractometer with graphite monochromated Mo- K_{α} radiation ($\lambda = 0.71073 \text{ \AA}$) using the SMART and SAINT programs. The structures were solved by direct methods and refined on F^2 by full-matrix least-squares methods with SHELXTL version 5.1. All non-hydrogen atoms were refined anisotropically. In **DPCP 2**, one S and one C atoms are positional disorder and occupy the same position. Crystallographic data for **DPCP 1–3** have been deposited in the Cambridge Crystallographic Data Centre with reference numbers CCDC 1052061–1052063. A summary of the crystallographic data and structure refinements of **DPCP 1–3** are tabulated in Table S1. The selected bond lengths and angles for **DPCP 1–3** are listed in Table S2.

2.2.5. OLED fabrication and measurements

Before device fabrication, the emitting complexes of **DPCP 3**, [1,4-bis[(1-naphthyl)phenyl]amino]-biphenyl (NPB) [25] and [bis(2-(2-hydroxyphenyl)-pyridine)beryllium] (Bepp₂) [26] were prepared and purified by sublimation, and ITO glass substrates were pre-cleaned carefully and treated by UV/O₃ for 2 min. The

devices were prepared in vacuum at a pressure of 5×10^{-6} Torr. All organics were thermally evaporated at a rate of 1.0 \AA s^{-1} at a base pressure of around 3.5×10^{-4} Pa. A LiF layer (0.5 nm) was deposited at a rate of 0.2 \AA s^{-1} . The finishing Al electrode (cathode) was



(a)

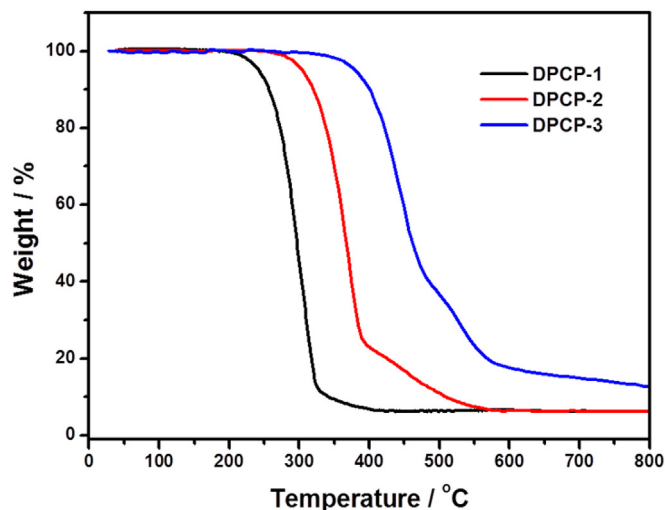
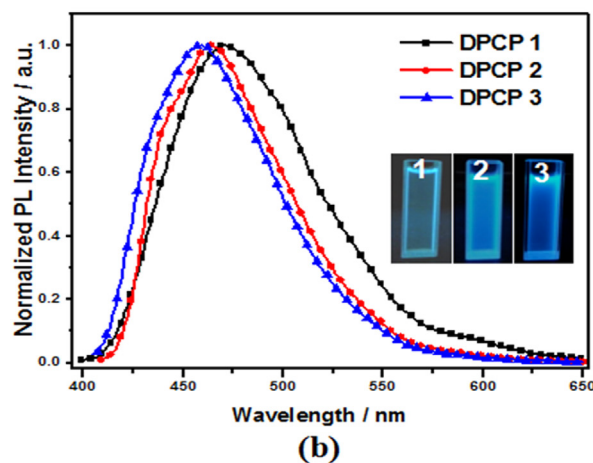


Fig. 1. The TGA curves of DPCP 1–3.



(b)

Fig. 2. UV–vis absorption (a) and photoluminescence (b) spectra of **DPCP 1–3** in CH_2Cl_2 solution ($5 \times 10^{-5} \text{ M}$). Inset: fluorescent images of **DPCP 1–3** in CH_2Cl_2 solutions under 365 nm UV irradiation.

Table 1
Photophysical properties and energy levels of **DPCP 1–3**.

	$\lambda_{\text{abs}}^{\text{a}}/\text{nm}$	$\lambda_{\text{em}}^{\text{a}}/\text{nm}$	$\lambda_{\text{em}}^{\text{b}}/\text{nm}$	$\Phi_{\text{F}}^{\text{a}}(\%)$	$\Phi_{\text{F}}^{\text{c}}(\%)$	$\Phi_{\text{F}}^{\text{d}}(\%)$	$\Phi_{\text{F}}^{\text{e}}(\%)$	$\Delta E_{\text{g}}/\text{eV}^{\text{f}}$	$E_{\text{LUMO}}/\text{eV}$	$E_{\text{HOMO}}/\text{eV}$
DPCP 1	368	471	483	8.96	1.28	1.52	1.89	2.92	-2.14	-5.06
DPCP 2	370	465	491	31.82	15.73	2.24	2.18	2.90	-2.21	-5.10
DPCP 3	366	457	475	37.28	16.2	24.61	26.12	2.94	-2.38	-5.32

^a Measured in dichloromethane solution (5×10^{-5} M).

^b Measured in powder.

^c Measured in acetone (5×10^{-5} M).

^d Measured in water/acetone mixtures (5×10^{-5} M).

^e Measured in film.

^f Data obtained from CV.

deposited at a rate of 10 \AA s^{-1} in another chamber. The thicknesses of the organic materials and the cathode layers were controlled using a quartz crystal thickness monitor. The electrical characteristics of the devices were measured with a Keithley 2400 source meter. The EL spectra and luminance of the devices were obtained on a PR650 spectrometer. All the devices fabrication and device characterization steps were carried out at room temperature under ambient laboratory conditions. Current-Voltage characteristics of single-carrier devices were measured using the same semiconductor parameter analyzer as for OLEDs.

3. Results and discussion

3.1. Synthesis

The synthetic route for **DPCP 1–3** and their chemical structures are shown in Scheme 1. The intermediates 1,3,5-triaryl-1,5-pentanediones obtained from the aldol condensation reaction of appropriate aryl aldehydes and acetyl benzene were cyclized in Zn/CH₃COOH system and dehydrated in the presence of concentrated hydrochloric acid to give 1,2-diphenyl-4-thiophenyl-1,3-cyclopentadiene (**DPCP 1**) as yellow solid in good yields of 78%. **DPCP 2** and **DPCP 3** were readily prepared via Suzuki coupling reactions between 1,2-diphenyl-4-(4-bromophenyl)-1,3-cyclopentadiene and corresponding boric acid in the presence of K₂CO₃ as base source and Pd(PPh₃)₄ as catalyst with yields of 76% and 85%, respectively. The products were purified by column chromatography on silica gel using dichloromethane–petroleum

ether as eluent. The structures were characterized by elemental analyses, ¹H NMR, ¹³C NMR, MS and single-crystal X-ray diffraction. All of three compounds have good solubility in most organic solvents at room temperature, such as n-hexane, dichloromethane, tetrahydrofuran, acetonitrile and methanol.

3.2. Thermal and optical properties

The thermal properties of the compounds were carried out by thermal gravimetric analysis (TGA) (Fig. 1) and by differential scanning calorimetry (DSC) (Fig. S1). The decomposition temperatures (T_{d}) were around 239, 317 and 383 °C for **DPCP 1**, **DPCP 2** and **DPCP 3**, respectively. It is very clear that T_{d} increase in the order of molecular weight. DSC measurements were examined under the nitrogen atmosphere. As shown in Table S3 and Fig. S1, all three compounds have high melting points (94 °C, 208 °C and 130 °C for **DPCP 1**, **DPCP 2** and **DPCP 3**, respectively) upon the first heating process. Only the glass transition temperatures were observed upon the second heating process which indicated an extreme tendency toward amorphous state of synthesized compounds [27]. **DPCP 2** and **DPCP 3** exhibited glass transition temperature (T_{g}) at 52 and 95 °C, respectively. Compared with **DPCP 1** and **DPCP 2**, **DPCP 3** showed a higher T_{g} and T_{d} values. This result proved to be the advantage of the series of **DPCP** derivatives in terms of thermal stabilities, especially for **DPCP 3**, which can prevent them from decomposing during the process of vacuum deposition as well as device working.

The UV–vis absorption and the photoluminescent (PL) spectra of **DPCP 1**, **DPCP 2** and **DPCP 3** in dilute solutions (5×10^{-5} M) are shown in Fig. 2 and the corresponding data are summarized in Table 1. Intense and similar absorption bands were observed in the ultraviolet part of the spectrum between 320 and 400 nm, assigning to the spin-allowed $\pi-\pi^*$ transition of the

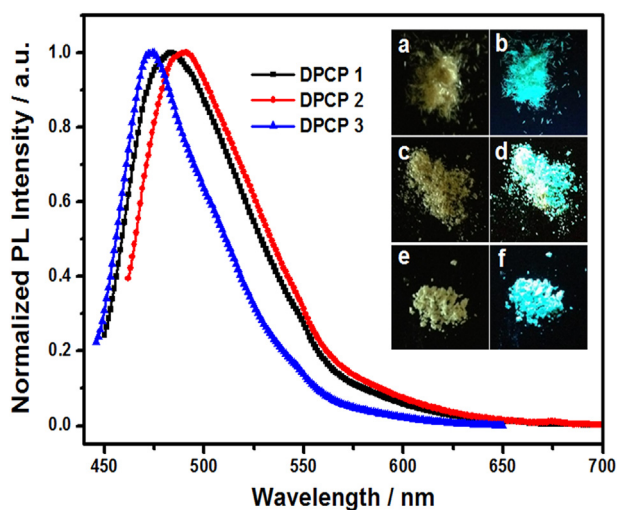


Fig. 3. Photoluminescence (PL) spectra of **DPCP 1–3** in powders. Inset: photographic images of powders **DPCP 1** (a and b), **DPCP 2** (c and d) and **DPCP 3** (e and f) under daylight (a, c, e) and 365 nm UV irradiation (b, d, f), respectively.

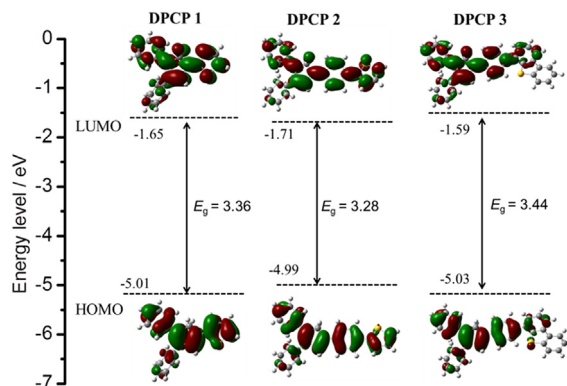


Fig. 4. Energy level alignment and pictorial drawings of HOMO and LUMO of **DPCP 1–3**.

cyclopentadiene moiety and conjugated backbone structure. The other absorption band at about 270 nm was attributed to the cyclopentadiene unit. The UV–vis absorption of 1,2,4-triphenylcyclopenta-1,3-diene [21b] also exhibited two distinct bands at 266 and 352 nm (Fig. S2). The first band of the absorption spectra of **DPCP 2** was red-shifted compared with that of **DPCP 1** because of the addition of another phenyl group. Their UV–vis absorption in solvents with different polarities such as n-hexane,

dichloromethane, THF, acetonitrile and methanol had also been investigated (Fig. S3). Apparently, the maximal absorption intensity increased and the fluorescence quantum yields mainly decreased with the increase of the solvent polarity.

As shown in Fig. 2b, three compounds showed blue PL emission with the maximum wavelength at 471, 465, and 457 nm in the dilute solution, respectively. Fluorescent peaks of **DPCP 1–3** exhibited slight red-shifts and the fluorescent intensity decreased

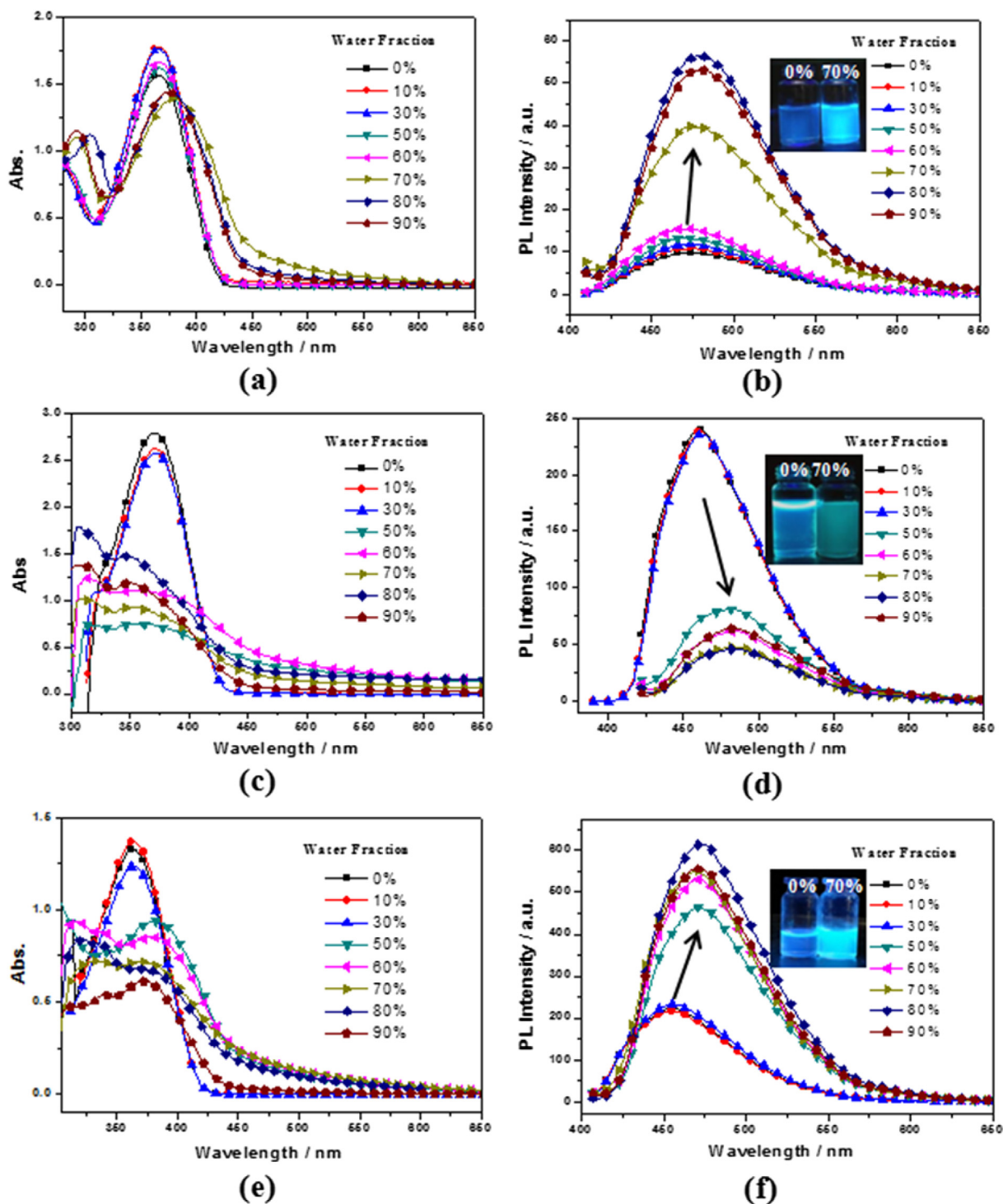


Fig. 5. UV–vis absorption and photoluminescence (PL) spectra of **DPCP 1** (a, b), **DPCP 2** (c, d) and **DPCP 3** (e, f) in water/acetone mixtures with different volume fractions of water. Concentration: 5×10^{-5} M.

in polar solvents compared with those in low polar ones (Fig. S3). This indicated that the polarity of the excited state is lower than that of the ground state of the compounds. All the compounds in the solid state also exhibit strong blue PL emission with the different degree red-shifted compared with those in solutions (Fig. 3). Furthermore, the fluorescence intensity and fluorescence quantum yields strengthened gradually from **DPCP 1** to **DPCP 3**. The detailed data are summarized in Table 1. According to the above analysis, **DPCP 3** shows bright blue emission in both solution and solid state with the highest fluorescence quantum yields.

3.3. Electrochemical properties and theoretical calculation

The electrochemical properties of **DPCP 1–3** were investigated by cyclic voltammetry (CV) which employed a conventional three-electrode cell containing a Pt working electrode, a glassy carbon counter electrode and an Ag/AgCl reference electrode. The CV curves of compounds are shown in Fig. S4. All of the compounds **DPCP 1–3** displayed oxidation peaks in the CV diagrams. The HOMO energy levels were obtained from the onset oxidation potentials. The energy band gaps (ΔE_g) of the compounds were estimated from the onset wavelength of the UV absorptions. The LUMO energy levels were determined from the HOMO energy together with energy band gap. The resulting data are also summarized in Table 1 and the HOMO levels are in the region of -5.06 to 5.32 eV. These are very closed to the work function of ITO anode [28], which

is favorable for hole injection and transportation in OLEDs. Among the three compounds, the oxidation peak of **DPCP 3** exhibited the highest potential. This indicated that **DPCP 3** need the highest energy to remove an electron out of its HOMO. In agreement with the case in the absorption spectra, the peak blue-shift is the result of the decreased HOMO level of **DPCP 3**.

To further investigate the origin of the highest occupied molecular orbital (HOMO) and lowest unoccupied molecular orbital (LUMO) levels, quantum mechanical computations were carried out with the optimized geometry using the Gaussian 09 program at the B3LYP/6-31G level. The plots and data of HOMOs and LUMOs are shown in Fig. 4. The LUMOs and the electron clouds of the HOMOs of **DPCP 1** and **DPCP 2** dispersed on the whole molecules, showing the weak intramolecular charge transfer of these compounds. On the HOMO orbital of **DPCP 3**, the electron cloud is mainly located at the central cyclopentadiene core and surrounding aromatic rings as well as sulfur atom in dibenzothiophene. The electron cloud in LUMO level was mainly composed of π and π^* orbitals of the cyclopentadiene and aromatic rings, showing electron-donating character of dibenzothiophene.

3.4. AIEE properties

To confirm the possible AIEE properties of all compounds, their fluorescent behaviors with water added into acetone were studied [29]. The UV–vis absorption and PL spectra for **DPCP 1–3** in the

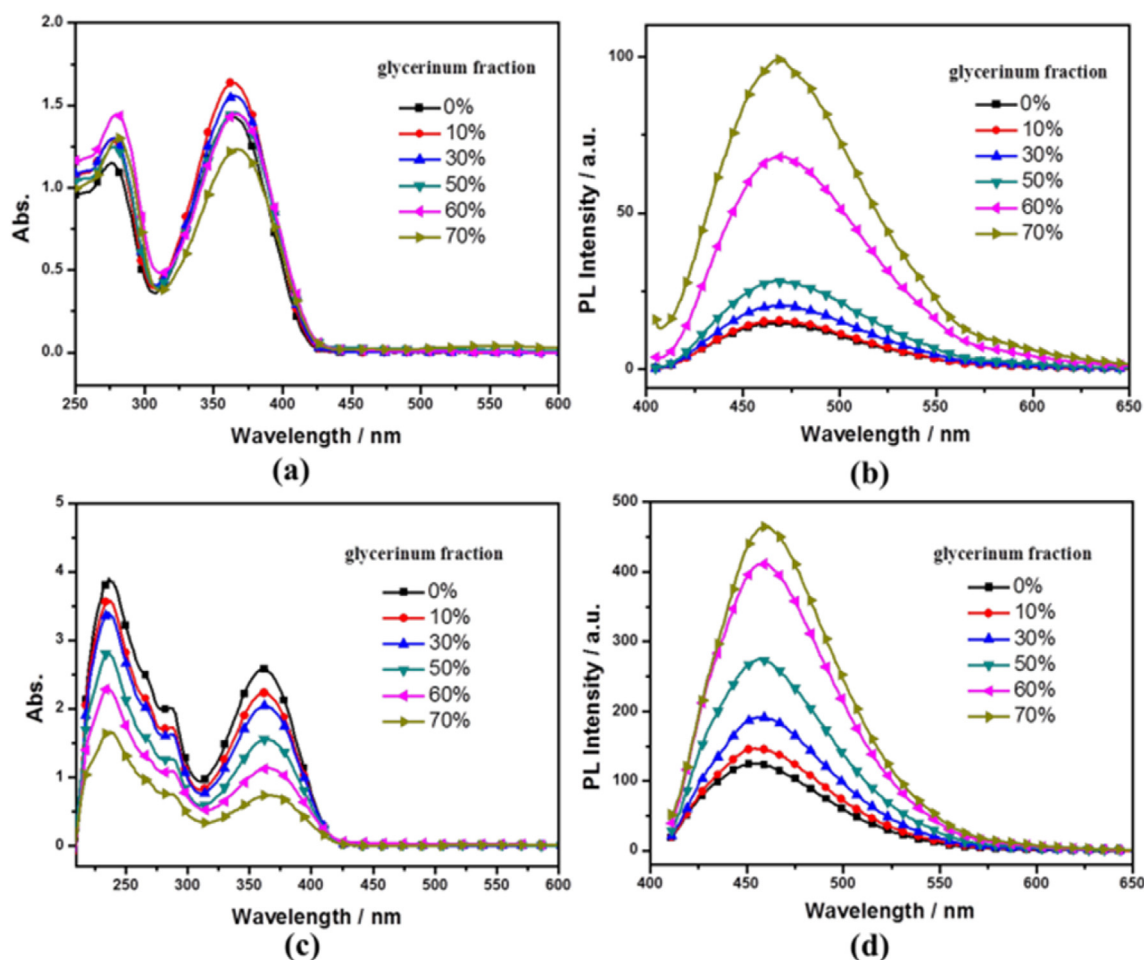


Fig. 6. UV–vis absorption and photoluminescence (PL) spectra of **DPCP 1** (a, b) and **DPCP 3** (c, d) in glycerol–methanol mixtures with different volume fractions of glycerol. Concentration: 5×10^{-5} M.

Table 2
The dihedral angles of the selected planes of the compounds.

	Dihedral angle/ $^{\circ}$			
	P ₁ –P ₂	P ₁ –P ₃	P ₁ –P ₄	P ₄ –P ₅
DPCP-1-I	55.80	27.39	25.59	–
DPCP-1-II	61.90	31.46	16.14	–
DPCP-2-I	39.41	39.41	29.48	3.59
DPCP-2-II	40.51	40.51	5.88	21.13
DPCP-3	61.58	31.76	7.00	37.35

water/acetone mixtures with different volume proportion are shown in Fig. 5. From the absorption spectra we can see that a level-off tail caused by the formation of aggregates was seen in the visible spectral region when the water fraction was over 50%. In addition, both **DPCP 1** and **DPCP 3** displayed an obvious red-shift with increasing water contents, which indicated the capable formation of *J*-aggregation [28]. On the contrary, **DPCP 2** displayed the opposite effect with blue-shift in the absorption spectra. Such phenomenon is the characteristic of the formation of *H*-aggregation [10]. In the PL spectra, the emission intensities kept unchanged when the water fraction was in the range 0–60% for **DPCP 1** and 0–30% for **DPCP 3**, then dramatically increased with the continued addition of water and the maximum wavelength was red-shifted to a certain extent. However, with the increase of water fraction, PL intensity for **DPCP 2** decreased and the maximal emission peak moved to longer wave which can be interpreted as fluorescence caused quenching.

To explore whether or not restriction of intramolecular rotation is responsible for AIEE of **DPCP 1** and **DPCP 3**, their fluorescence

spectra in a mixture of methanol and glycerol, with different volume proportion was tested (Fig. 6) [30]. The emission intensities drastically increased on the continued addition of glycerol. It indicated that glycerol restricted the rotation of single bond of the molecules, thus generating AIEE phenomenon.

3.5. Crystal structures

In order to further understand the relationship between photophysical properties and structures, the single crystals of compounds **DPCP 1–3** were successfully obtained from dichloromethane/methanol mixtures. Single crystal X-ray analysis revealed that **DPCP 1–3** crystallize in orthorhombic crystal system with space group *Pna2₁*, *Fdd2* and *Pca2₁*, respectively (Table S1). All molecules adopted non-coplanar conformations and possessed different packing patterns because of strict repulsion which can influence some of their electronic and physical properties such as a suppression of the conjugation [31]. Table 2 gives the selected dihedral angles between the substituent moieties and central cyclopentadiene ring of the three compounds. As shown in Fig. 7a, there are two constituent molecules (I and II) in the asymmetric unit of **DPCP 1**. Two phenyl rings and one thiophenyl ring are forced to twist out of the cyclopentadiene plane with dihedral angles in the range 55.80°, 27.39° and 25.59°, respectively. Interestingly, the spiral chain structure (Fig. 7b) derives from the weak C–H... π interactions between adjacent II-type single molecules. These chains and I-type molecules are further packed without strong aromatic π ... π interactions (Fig. 7c). This packing structure could improve the fluorescence intensity in aggregation state.

In **DPCP 2**, the molecule has two different spatial conformations, **DPCP 2-I** and **DPCP 2-II** (Fig. 8a). Two phenyl rings connected with

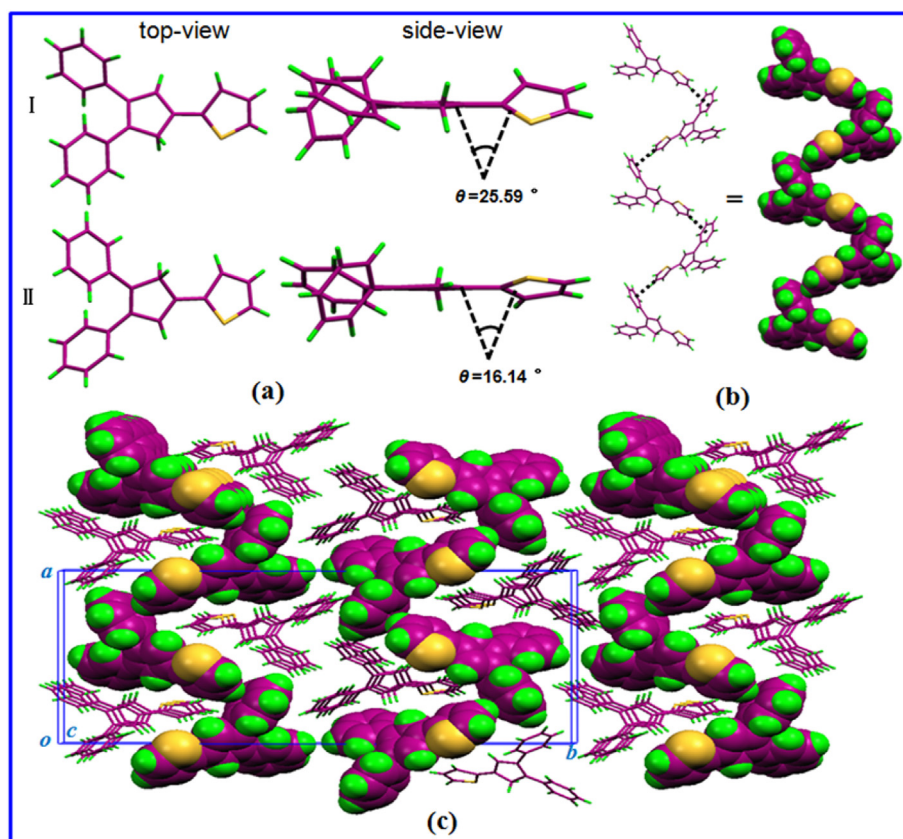


Fig. 7. (a) Crystal structure of **DPCP 1**, (b) spiral chain structure and (c) packing arrangements in the crystal of **DPCP 1**. The dotted line represented C–H... π interactions.

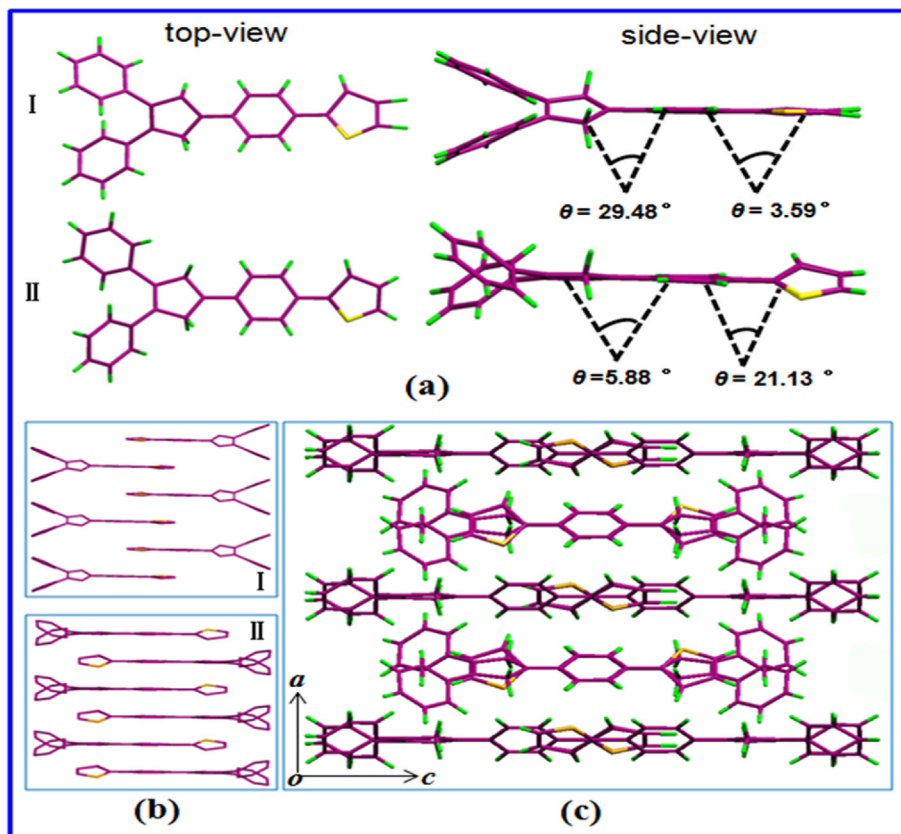


Fig. 8. Molecular structures (a) and packing arrangements (b and c) in the crystal structure of DPCP 2.

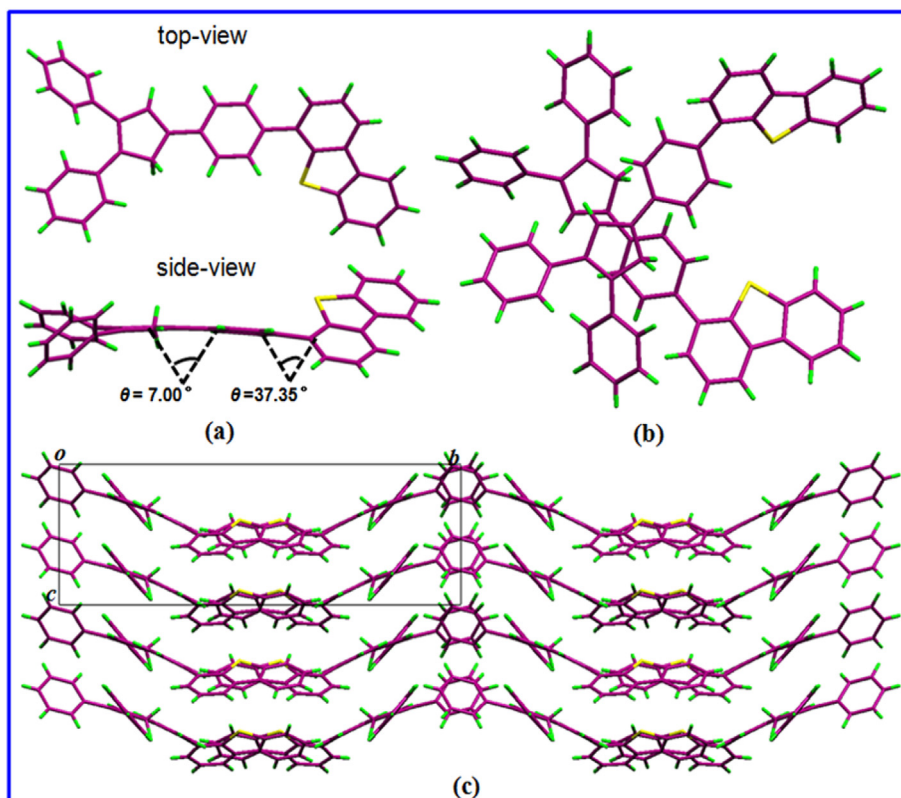


Fig. 9. Molecular structures (a), dimer structure (b) and packing arrangements (c) in the crystal structure of DPCP 3.

cyclopentadiene core were twisted out with dihedral angles in the range of 31.46–39.41°. The dihedral angle (3.59°) between thiophenyl ring and neighboring phenyl rings in **DPCP 2-I** is smaller than that (21.13°) in **DPCP 2-II**. Compared with **DPCP 1**, the effective conjugation length in the molecule was increased by using 4-thiophenyl-phenyl to replace thiophenyl moieties. As shown in Fig. 8b, both **DPCP 2-I** and **DPCP 2-II** columns were formed. There is no noteworthy intermolecular $\pi\cdots\pi$ interaction within each molecular column, but alike *H*-aggregate enables the compound to have AIEE-inactive characteristics.

The molecular structure and packing structure of **DPCP 3** are shown in Fig. 9. The dihedral angle between the central cyclopentadiene plane and the connector benzene plane is only 7.00°, and terminal 4-dibenzothiophene plane has certain distortions from the bulky conjugation skeletons with dihedral angles of 37.35°. There is aromatic C-H $\cdots\pi$ interactions among adopt parallel arrangement model with two kinds of molecular two single molecules with an interaction distance of 2.97 Å to form a dimer (Fig. 9b) as *X*-aggregates which could increase the resistance between molecules. There are no strong aromatic $\pi\cdots\pi$ interactions because the center–center distance between two molecules is 8.473 Å along *b*-axis. This structure feature further avoided the maximum face-to-face stacking (Fig. 9c) to improve the fluorescence intensity in aggregation state. According to crystal structures and the spectroscopy, the AIEE properties of **DPCP 1**, **DPCP 3** should be attributed to combined effects of restricted intramolecular rotation (RIR) and the formation of *J*- and *X*-aggregations.

3.6. Electroluminescent properties

DPCP 3 with the highest fluorescence quantum yield as well as high thermal stability indeed has the potential as blue-emitting material. To evaluate the EL performance of **DPCP 3**, a non-doped OLED with a simple configuration of [ITO/NPB (20 nm)/**DPCP 3**

(30 nm)/Bepp₂ (50 nm)/LiF (10 nm)/Al (200 nm)] was fabricated. The device configuration and the energy diagram of the materials used in the EL device above are shown in Fig. 10a and b. NPB and Bepp₂ were employed as the hole transport layer (HTL) and electron transport layer (ETL), respectively, and the neat film **DPCP 3** was adopted as the emitting layer (EML). Fig. 10c shows the EL spectrum of this device at the brightness of 100 cd m⁻². It shows the emission peak at around 462 nm with the Commission Internationale de l'Éclairage (CIE_{x,y}) coordinates of (0.16, 0.16) and remain almost unchanged in the driving voltage range from 4 V to 8 V as shown in Fig. 10d, which is consistent well with the PL spectral characteristics of this compound. The current density–voltage–luminance (*J*–*V*–*L*) characteristics and the luminance efficiency (LE) and power efficiency (PE) plotted with respect to the voltage of the device are shown in Fig. S5. All the devices displayed low driving voltages, and the corresponding current density and luminance exhibited sustained increase upon increasing driving voltage. The quite low turn-on voltage about 3.2 V was realized due to the easily charge injection from the HTL and/or ETL into the EML. The driving voltage for the luminance of 100 cd m⁻² is 5.1 V and the maximum luminance of 2277 cd m⁻² is obtained at 8.5 V. More importantly, the LE and PE values of 0.42 cd A⁻¹ and 0.26 lm W⁻¹ were achieved at the practical luminance of 100 cd m⁻². Such EL performance is comparable to the non-doped blue OLEDs based on cyclopentadiene derivatives with a maximum luminance 950 cd m⁻² [19]. Although there is no optimization of device configurations, but **DPCP 3** shows good performance.

4. Conclusions

In conclusion, we have successfully designed and simply synthesized three cyclopentadiene derivatives by introducing thiophene ring and dibenzothiophene group. **DPCP 1** and **DPCP 3** exhibited typical AIEE character as a result of the combined effects

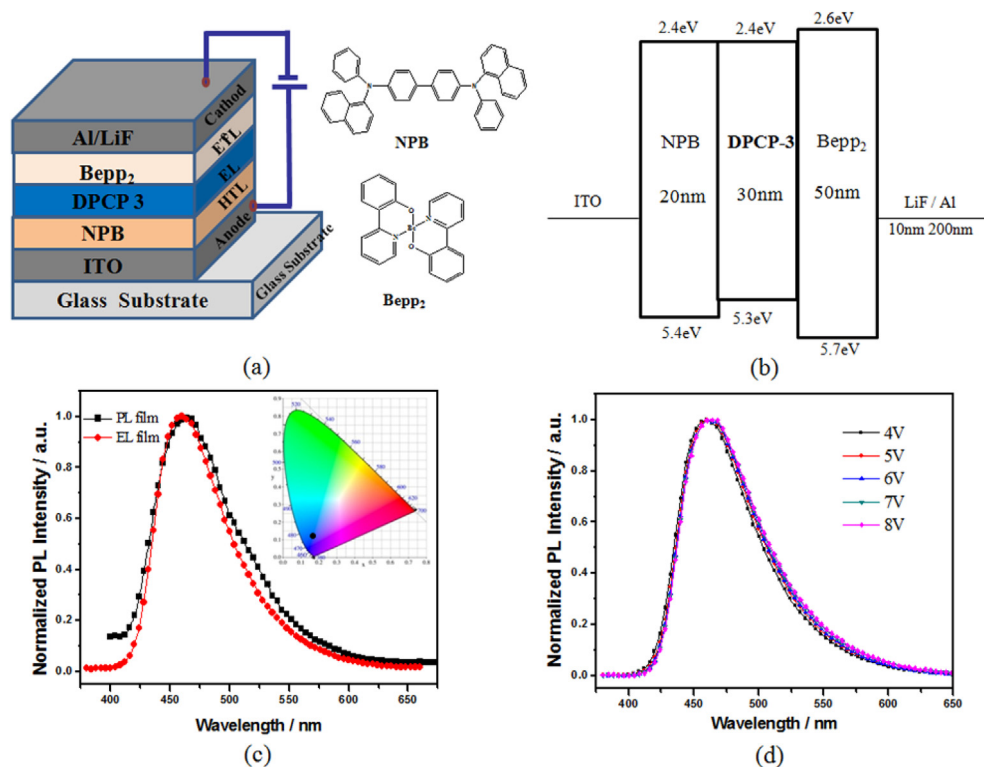


Fig. 10. (a) The EL device structure and the chemical structure of NPB and Bepp₂; (b) the energy level diagram of the materials in EL device; (c) EL, PL spectra and CIE coordinates of device (inset); (d) EL spectra of devices at different applied voltages.

of restricted intramolecular rotation (RIR) and the formation of J- and X-aggregations. These compounds emit strong blue fluorescence both in solutions and in powders. In addition, they showed high thermal stability with the decomposition temperature of 239–363 °C and appropriate energy levels with the region of 5.06–5.32 eV which is favorable for hole injection and transportation in OLEDs. Non-doped three-layer blue OLEDs based on **DPCP 3** has a high performance with a turn-on voltage of 3.2 V and the maximum luminance of 2277 cd m⁻² as well as the CIE coordinates of (0.16, 0.16). This work presents a promising approach for designing new luminescent materials with AIEE character and gives some efficient evidence for understanding the relationship between molecular structures and photophysical properties.

Acknowledgment

This work was supported by the National Natural Science Foundation of China (51003009), the Fundamental Research Funds for the Central Universities of China (DUT14LK32) and the Science and Technology Research Foundation of Education Department of Liaoning Province (L2014033).

Appendix A. Supplementary data

Supplementary data related to this article can be found at <http://dx.doi.org/10.1016/j.dyepig.2015.09.018>.

References

- [1] (a) D'Andrade BW, Forrest SR. White organic light-emitting devices for solid-state lighting. *Adv Mater* 2004;16:1585–95.
(b) Ye SH, Chen JM, Di C, Liu YQ, Lu K, Wu WP, et al. Phenyl-substituted fluorene-dimer cored anthracene derivatives: highly fluorescent and stable materials for high performance organic blue-and white-light-emitting diodes. *J Mater Chem* 2010;20:3186–94.
(c) Jung BJ, Yoon CB, Shim HK, Do LM, Zyung T, et al. Pure-red dye for organic electroluminescent devices: bis-condensed DCM derivatives. *Adv Mater* 2001;11:430–4.
(d) Zhu MR, Yang CL. Blue fluorescent emitters: design tactics and applications in organic light-emitting diodes. *Chem Soc Rev* 2013;42:4963–76.
(e) Gong SL, Sun N, Luo JJ, Zhong C, Ma DG, et al. Highly efficient simple-structure blue and all-phosphor warm-white phosphorescent organic light-emitting diodes enabled by wide-band gap tetraarylsilane-based functional materials. *Adv Funct Mater* 2014;24:5710–8.
- [2] (a) Huang ZY, Chiu SW, Chen CW, Chen YH, Lin LY, Wong KT, et al. Spontaneous formation of light-trapping nano-structures for top-illumination organic solar cells. *Nanoscale* 2014;6:2316–20.
(b) Harafuji K, Sato H, Matsuura T, Omoto Y, Kaji T, Hiramoto M, et al. Degradation in organic solar cells under illumination and electrical stresses in air. *Jpn J Appl Phys* 2014;53:122303.
- [3] (a) Chen CP, Huang CY, Chuang SC. Organic photovoltaics: highly thermal stable and efficient organic photovoltaic cells with crosslinked networks appending open-cage fullerenes as additives. *Adv Funct Mater* 2015;25:206.
(b) Atkin P, Farid MM. Improving the efficiency of photovoltaic cells using PCM infused graphite and aluminium fins. *Sol Energy* 2015;114:217–28.
(c) Ottono C, Berrouard P, Louarn G, Beaupré S, Gendron D, Zaqorska M, et al. Donor–acceptor alternating copolymers containing thienopyrroledione electron accepting units: preparation, redox behaviour, and application to photovoltaic cells. *Polym Chem* 2012;3:2355–65.
- [4] (a) Xu JP, Fang Y, Song ZG, Mei J, Jia L, Qin AJ, et al. BSA–tetraphenylethene derivative conjugates with aggregation-induced emission properties: fluorescent probes for label-free and homogeneous detection of protease and α 1-antitrypsin. *Analyst* 2011;136:2315–21.
(b) Fan Z, Zhou H, Li PY, Speer JE, Cheng H, et al. Structural elucidation of cell membrane-derived nanoparticles using molecular probes. *J Mater Chem B* 2014;2:8231–8.
(c) Zhao J, Ji S, Chen Y, Guo HM, Yang P, et al. Excited state intramolecular proton transfer (ESIPT): from principal photophysics to the development of new chromophores and applications in fluorescent molecular probes and luminescent materials. *Phys Chem Chem Phys* 2012;14:8803–17.
- [5] (a) van de Linde S, Sauer M. How to switch a fluorophore: from undesired blinking to controlled photoswitching. *Chem Soc Rev* 2014;43:1076–87.
(b) Gaillard C, Adumeau P, Canet JL, Gautier A, Boyer D, Beaudoin C, et al. Monodisperse silica nanoparticles doped with dipicolinic acid-based luminescent lanthanide (III) complexes for bio-labelling. *J Mater Chem B* 2013;1:4306–12.
- [6] Li C, Yan H, Zhao LX, Zhang GF, Hu Z, Huang ZL, et al. A trident dithienylethene-perylenemonoimide dyad with super fluorescence switching speed and ratio. *Nat Commun* 2014;5:5709–19.
- [7] (a) Chen CT. Evolution of red organic light-emitting diodes: materials and devices. *Chem Mater* 2004;16:4389–400.
(b) Yang MD, Zhang Y, Zhu WJ, Wang HZ, Huang J, Cheng LH, et al. Difunctional chemosensor for Cu(II) and Zn(II) based on Schiff base modified anthryl derivative with aggregation-induced emission enhancement and piezochromic characteristics. *J Mater Chem C* 2015;3:1994–2002.
(c) Zhang Y, Haske W, Cai D, Barlow S, Kippelen B, Marder S. Efficient blue-emitting electrophosphorescent organic light-emitting diodes using 2-(3,5-di(carbazol-9-yl) phenyl)-5-phenyl-1, 3, 4-oxadiazole as an ambipolar host. *RSC Adv* 2013;3:23514–20.
- [8] (a) Chan LH, Lee RH, Hsieh CF, Yeh HC, Chen CT. Optimization of high-performance blue organic light-emitting diodes containing tetraphenylsilane molecular glass materials. *J Am Chem Soc* 2002;124:6469–79.
(b) Zeng Q, Li Z, Dong YQ, Di CA, Qin AJ, Hong YN, et al. Fluorescence enhancements of benzene-cored luminophors by restricted intramolecular rotations: AIE and AIEE effects. *Chem Commun* 2007:70–2.
(c) Yuan WZ, Lu P, Chen S, Lam JWY, Wang ZM, Liu Y, et al. Changing the behavior of chromophores from aggregation-caused quenching to aggregation-induced emission: development of highly efficient light emitters in the solid state. *Adv Mater* 2010;22:2159–63.
(d) Tang X, Yao L, Liu H, Shen FZ, Zhang ST, Zhang HH, et al. An efficient AIE-active blue-emitting molecule by incorporating multifunctional groups into tetraphenylsilane. *Chem Eur J* 2014;20:7589–92.
- [9] Luo JD, Xie ZL, Lam JWY, Cheng L, Chen HY, Qiu CF, et al. Aggregation-induced emission of 1-methyl-1, 2, 3, 4, 5-pentaphenylsilole. *Chem Commun* 2001;18:1740–1.
- [10] An BK, Kwon SK, Jung SD, Park SY. Enhanced emission and its switching in fluorescent organic nanoparticles. *J Am Chem Soc* 2002;124:14410–5.
- [11] (a) Barr JW, Bell TW, Catalano VJ, Cline JL, Phillips DJ, Procupez R. Syntheses, structures, and photoisomerization of (E)- and (Z)-2-tert-butyl-9-(2, 2, 2-triphenylethylidene) fluorene. *J Phys Chem A* 2005;109:11650–4.
(b) Huang J, Sun N, Yang J, Tang R, Li QQ, Ma DG, et al. Blue aggregation-induced emission luminogens: high external quantum efficiencies up to 3.99% in LED device, and restriction of the conjugation length through rational molecular design. *Adv Funct Mater* 2014;24:7645–54.
(c) Huang J, Jiang Y, Yang J, Tang R, Xie N, Li QQ, et al. Construction of efficient blue AIE emitters with triphenylamine and TPE moieties for non-doped OLEDs. *J Mater Chem C* 2014;2:2028–36.
- [12] (a) Chen J, Law CCW, Lam JWY, Dong YP, Lo SMF, Williams LD, et al. Synthesis, light emission, nanoaggregation, and restricted intramolecular rotation of 1, 1-substituted 2, 3, 4, 5-tetraphenylsiloles. *Chem Mater* 2003;15:1535–46.
(b) Zhang P, Wang HT, Liu HM, Li M. Fluorescence-enhanced organogels and mesomorphic superstructure based on hydrazine derivatives. *Langmuir* 2010;26:10183–90.
- [13] (a) Qian G, Dai B, Luo M, Yu DB, Zhan J, Zhang ZQ, et al. Band gap tunable, donor–acceptor–donor charge-transfer heteroquinoid-based chromophores: near infrared photoluminescence and electroluminescence. *Chem Mater* 2008;20:6208–16.
(b) Qian Y, Li SY, Zhang GQ, Wang Q, Wang SQ, Xu HJ, et al. Aggregation-induced emission enhancement of 2-(2'-hydroxyphenyl) benzothiazole-based excited-state intramolecular proton-transfer compounds. *J Phys Chem B* 2007;111:5861–8.
(c) Huang C, Barlow S, Marder SR. Perylene-3, 4, 9, 10-tetracarboxylic acid diimides: synthesis, physical properties, and use in organic electronics. *J Org Chem* 2011;8:2386–407.
- [14] (a) Feng X, Hu JY, Iwanaga F, Seto N, Redshaw C, Elsegood MRJ, et al. Blue-emitting butterfly-shaped 1, 3, 5, 9-tetraarylpyrenes: synthesis, crystal structures, and photophysical properties. *Org Lett* 2013;15:1318–21.
(b) Zhang Y, Ng TW, Lu F, Tong QX, Lai SL, Chan MY, et al. A pyrene-phenanthroimidazole derivative for non-doped blue organic light-emitting devices. *Dyes Pigments* 2013;98:190–4.
- [15] (a) Sato T, Jiang DL, Aida T. A blue-luminescent dendritic rod: poly(phenyleneethynylene) within a light-harvesting dendritic envelope. *J Am Chem Soc* 1999;121:10658–9.
(b) Zhao QL, Zhang S, Liu Y, Mei J, Chen SJ, Lu P, et al. Tetraphenylethynyl-modified perylenebisimide: aggregation-induced red emission, electrochemical properties and ordered microstructures. *J Mater Chem* 2012;22:7387–94.
(c) Zhang QC, Divayana Y, Xiao JC, Wang ZJ, Tiekink ERT, Doung HM, et al. Synthesis, characterization, and bipolar transporting behavior of a new twisted polycyclic aromatic hydrocarbon: 1',4'-diphenyl-naphtho-(2',3':1,2)-pyrene-6'-nitro-7'-methyl carboxylate. *Chem Eur J* 2010;25:7422–6.
- [16] Adachi C, Tsutsui T, Saito S. Blue light-emitting organic electroluminescent devices. *Appl Phys Lett* 1990;56:799–801.
- [17] Yoshino K, Tada K, Hirohata M, Kajii H, Hironaka Y, Tada N, et al. Novel properties of molecularly doped conducting polymers and junction devices. *Synth Met* 1997;84:477–82.
- [18] Zhao YS, Fu H, Hu F, Peng AD, Yao J. Multicolor emission from ordered assemblies of organic 1D nanomaterials. *Adv Mater* 2007;19:3554–8.
- [19] Gao XC, Cao H, Huang L, Huang YY, Zhang BW, Huang CH. Comparison of the electroluminescence and its related properties of two cyclopentadiene derivatives. *Appl Sur Sci* 2003;210:183–9.

- [20] Ohmori Y, Hironaka Y, Yoshida M, Fujii A, Yoshino K. Enhancement of electroluminescence intensity from dye-doped poly(3-alkylthiophene) light emitting diode with different alkyl-side-chain length. *Jpn J Appl Phys* 1996;35:4105–9.
- [21] (a) Yang LJ, Ye JW, Xu LF, Yang XY, Gong WT, Lin Y, et al. Synthesis and properties of aggregation-induced emission enhancement compounds derived from triarylcyclopentadiene. *RSC Adv* 2012;2:11529–35.
(b) Zhang XD, Ye JW, Xu LF, Yang LJ, Deng D, Ning GL. Synthesis, crystal structures and aggregation-induced emission enhancement of aryl-substituted cyclopentadiene derivatives. *J Lumin* 2013;139:28–34.
(c) Ning GL, Li XC, Munakata M, Gong WT, Maekawa M, Kamikawa T. Conversion of phenyl-substituted cyclopentadienes to pyrylium cations. *J Org Chem* 2004;69:1432–4.
(d) Zhang XD, Ye JW, Wang SN, Gong WT, Lin Y, Ning GL. Heterocyclic radical mediated synthesis and fluorescence properties of conjugated polyene ketones. *Org Lett* 2011;13:3608–11.
(e) Yang LJ, Ye JW, Gao Y, Deng D, Lin Y, Ning GL. One-step stereoselective synthesis of (2Z, 4Z, 6Z, 8Z)-decatetraene diketone from pyrylium salts. *Eur J Org Chem* 2014;3:515–22.
- [22] (a) Jeong SH, Lee JY. Dibenzothiophene derivatives as host materials for high efficiency in deep blue phosphorescent organic light emitting diodes. *J Mater Chem* 2011;21:14604–9.
(b) Huang TH, Whang WT, Shen JY, Lin JT, Zheng HG. Organic electroluminescent derivatives containing dibenzothiophene and diarylamine segments. *J Mater Chem* 2005;15:3233–40.
- [23] (a) Dawson WR, Windsor MW. Fluorescence yields of aromatic compounds. *J Phys Chem* 1968;72:3251–60.
(b) Crosby GA, Demas JN. Measurement of photoluminescence quantum yields. *J Phys Chem* 1971;8:991–1024.
- [24] Huang C, Zhen CG, Su SP, Loh KP, Chen ZK. Solution-processable polyphenylphenyl dendron bearing molecules for highly efficient blue light-emitting diodes. *Org Lett* 2005;7:391–4.
- [25] Hirai Y, Uozumi Y. Clean synthesis of triarylaminines: Buchwald–Hartwig reaction in water with amphiphilic resin-supported palladium complexes. *Chem Commun* 2010;46:1103–5.
- [26] (a) Li YQ, Liu Y, Bu WM, Lu D, Wu Y, Wang Y. Hydroxyphenyl-pyridine beryllium complex (Bepp₂) as a blue electroluminescent material. *Chem Mater* 2000;12:2672–5.
(b) Liu Y, Guo JH, Feng J, Zhang HD, Li YQ, Wang Y. High-performance blue electroluminescent devices based on hydroxyphenyl-pyridine beryllium complex. *Appl Phys Lett* 2001;78:2300–2.
- [27] Shih PI, Chuang CY, Chien CH, Diao EWG, Shu CF. Highly efficient non-doped blue-light-emitting diodes based on an anthracene derivative end-capped with tetraphenylethylene groups. *Adv Funct Mater* 2007;17:3141–6.
- [28] (a) Li HY, Chi ZG, Xu BJ, Zhang XQ, Li XF, Liu SW, et al. Aggregation-induced emission enhancement compounds containing triphenylamine-anthrylenevinylene and tetraphenylethylene moieties. *J Mater Chem* 2011;21:3760–7.
(b) Hirata S, Kubota K, Jung HH, Hirata O, Goushi K, Yahiro M, et al. Improvement of electroluminescence performance of organic light-emitting diodes with a liquid-emitting layer by introduction of electrolyte and a hole-blocking layer. *Adv Mater* 2011;23:889–93.
- [29] Zhang XQ, Chi ZG, Li HY, Xu BJ, Li XF, Liu SW, et al. Synthesis and properties of novel aggregation-induced emission compounds with combined tetraphenylethylene and dicarbazolyltriphenylethylene moieties. *J Mater Chem* 2011;21:1788–96.
- [30] Kim KH, Bae SY, Kim YS, Hur JA, Hoang MH, Lee TW, et al. Highly photosensitive J-aggregated single-crystalline organic transistors. *Adv Mater* 2011;23:3095–9.
- [31] Prachumrak N, Namuangruk S, Keawin T, Jungsuttingwong S, Sudyoasuk T, Promarak V. Synthesis and characterization of 9-(fluoren-2-yl) anthracene derivatives as efficient non-doped blue emitters for organic light-emitting diodes. *Eur J Org Chem* 2013;2013:3825–34.